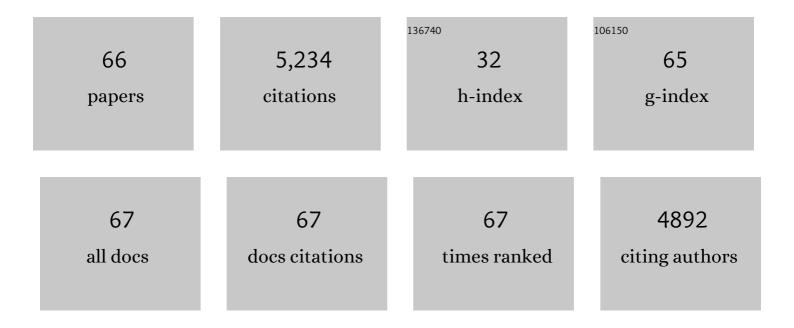
List of Publications by Year in descending order

Source: https://exaly.com/author-pdf/5307881/publications.pdf Version: 2024-02-01



Ромены Уш

#	Article	IF	CITATIONS
1	Facile synthesis of various Co3O4/bio-activated carbon electrodes for hybrid capacitor device application. Journal of Alloys and Compounds, 2022, 891, 161967.	2.8	22
2	Facile Synthesis of Amorphous MoCo Lamellar Hydroxide for Alkaline Water Oxidation. ChemSusChem, 2022, 15, .	3.6	4
3	Doping and interface engineering in a sandwich Ti ₃ C ₂ T _{<i>x</i>} /MoS _{2â^²<i>x</i>} P _{<i>x</i>} heterostructure for efficient hydrogen evolution. Journal of Materials Chemistry C, 2022, 10, 4140-4147.	2.7	26
4	Spatial porosity design of Fe–N–C catalysts for high power density PEM fuel cells and detection of water saturation of the catalyst layer by a microwave method. Journal of Materials Chemistry A, 2022, 10, 7764-7772.	5.2	11
5	Environmentally Tough and Stretchable MXene Organohydrogel with Exceptionally Enhanced Electromagnetic Interference Shielding Performances. Nano-Micro Letters, 2022, 14, 77.	14.4	91
6	3-D hierarchical urchin-like Fe3O4/CNTs architectures enable efficient electromagnetic microwave absorption. Materials Science and Engineering B: Solid-State Materials for Advanced Technology, 2022, 281, 115721.	1.7	14
7	lron atom–cluster interactions increase activity and improve durability in Fe–N–C fuel cells. Nature Communications, 2022, 13, .	5.8	159
8	Non-classical hydrogen storage mechanisms other than chemisorption and physisorption. Applied Physics Reviews, 2022, 9, .	5.5	16
9	Carbon Fibers Embedded with Aligned Magnetic Particles for Efficient Electromagnetic Energy Absorption and Conversion. ACS Applied Materials & Interfaces, 2021, 13, 5266-5274.	4.0	21
10	Hydrogen storage in incompletely etched multilayer Ti2CTx at room temperature. Nature Nanotechnology, 2021, 16, 331-336.	15.6	145
11	Efficient microwave absorber and supercapacitors derived from puffed-rice-based biomass carbon: Effects of activating temperature. Journal of Colloid and Interface Science, 2021, 594, 290-303.	5.0	99
12	Hydrogen Passivation of M–N–C (M = Fe, Co) Catalysts for Storage Stability and ORR Activity Improvements. Advanced Materials, 2021, 33, e2103600.	11.1	81
13	Hydrogen Passivation of M–N–C (M = Fe, Co) Catalysts for Storage Stability and ORR Activity Improvements (Adv. Mater. 38/2021). Advanced Materials, 2021, 33, 2170300.	11.1	17
14	Multiple reflection and scattering effects of the lotus seedpod-based activated carbon decorated with Co3O4 microwave absorbent. Journal of Colloid and Interface Science, 2021, 602, 344-354.	5.0	16
15	Plasmon-Enhanced Oxygen Evolution Catalyzed by Fe ₂ N-Embedded TiO _{<i>x</i>} N _{<i>y</i>} Nanoshells. ACS Applied Energy Materials, 2020, 3, 146-151.	2.5	18
16	Hierarchical Cobalt Selenides as Highly Efficient Microwave Absorbers with Tunable Frequency Response. ACS Applied Materials & amp; Interfaces, 2020, 12, 1222-1231.	4.0	62
17	Dielectric parameters of activated carbon derived from rosewood and corncob. Journal of Materials Science: Materials in Electronics, 2020, 31, 18077-18084.	1.1	14
18	Synergy between metallic components of MoNi alloy for catalyzing highly efficient hydrogen storage of MgH2. Nano Research, 2020, 13, 2063-2071.	5.8	64

#	Article	IF	CITATIONS
19	Carbon black-supported FM–N–C (FM = Fe, Co, and Ni) single-atom catalysts synthesized by the self-catalysis of oxygen-coordinated ferrous metal atoms. Journal of Materials Chemistry A, 2020, 8, 13166-13172.	5.2	27
20	Boosting electrocatalytic water splitting via metal-metalloid combined modulation in quaternary Ni-Fe-P-B amorphous compound. Nano Research, 2020, 13, 447-454.	5.8	77
21	Sequential Synthesis and Activeâ€Site Coordination Principle of Precious Metal Singleâ€Atom Catalysts for Oxygen Reduction Reaction and PEM Fuel Cells. Advanced Energy Materials, 2020, 10, 2000689.	10.2	92
22	Fe ₃ O ₄ Nanoflower-Carbon Nanotube Composites for Microwave Shielding. ACS Applied Nano Materials, 2019, 2, 5475-5482.	2.4	42
23	Surface-Oxidized Amorphous Fe Nanoparticles Supported on Reduced Graphene Oxide Sheets for Microwave Absorption. ACS Applied Nano Materials, 2019, 2, 4367-4376.	2.4	37
24	Magnetically induced abnormal grain growth in pure nickel. Materials Science and Technology, 2019, 35, 1533-1538.	0.8	0
25	Fe–N–C electrocatalyst with dense active sites and efficient mass transport for high-performance proton exchange membrane fuel cells. Nature Catalysis, 2019, 2, 259-268.	16.1	958
26	Recent advances in magnesium-based hydrogen storage materials with multiple catalysts. International Journal of Hydrogen Energy, 2019, 44, 10694-10712.	3.8	71
27	Antiferromagnetic Piezospintronics. Advanced Electronic Materials, 2019, 5, 1900176.	2.6	73
28	A layered double hydroxide-derived exchange spring magnet array grown on graphene and its application as an ultrathin electromagnetic wave absorbing material. Journal of Materials Chemistry C, 2019, 7, 12270-12277.	2.7	42
29	Multifunctional Organic–Inorganic Hybrid Aerogel for Selfâ€Cleaning, Heatâ€Insulating, and Highly Efficient Microwave Absorbing Material. Advanced Functional Materials, 2019, 29, 1807624.	7.8	458
30	Multiscale influence of trace Tb addition on the magnetostriction and ductility of <mml:math xmlns:mml="http://www.w3.org/1998/Math/MathML"><mml:mrow><mml:mo>â@©</mml:mo><mml:mn>100< oriented directionally solidified Fe-Ga crystals. Physical Review Materials, 2019, 3, .</mml:mn></mml:mrow></mml:math 	/monostmn>	≺nomml:mo>â(
31	Templateâ€Free Formation of Uniform Fe ₃ O ₄ Hollow Nanoflowers Supported on Reduced Graphene Oxide and Their Excellent Microwave Absorption Performances. Physica Status Solidi (A) Applications and Materials Science, 2018, 215, 1701049.	0.8	26
32	Yolk–shell structured Co-C/Void/Co9S8 composites with a tunable cavity for ultrabroadband and efficient low-frequency microwave absorption. Nano Research, 2018, 11, 4169-4182.	5.8	139
33	MWCNTs as Conductive Network for Monodispersed Fe ₃ O ₄ Nanoparticles to Enhance the Wave Absorption Performances. Advanced Engineering Materials, 2018, 20, 1700543.	1.6	50
34	Singleâ€Atom to Singleâ€Atom Grafting of Pt ₁ onto FeN ₄ Center: Pt ₁ @FeNC Multifunctional Electrocatalyst with Significantly Enhanced Properties. Advanced Energy Materials, 2018, 8, 1701345.	10.2	371
35	An Efficient Co/C Microwave Absorber with Tunable Co Nanoparticles Derived from a ZnCo Bimetallic Zeolitic Imidazolate Framework. Particle and Particle Systems Characterization, 2018, 35, 1800107.	1.2	47
36	Chemical Synthesis of High-Stable Amorphous FeCo Nanoalloys with Good Magnetic Properties. Nanomaterials, 2018, 8, 154.	1.9	26

#	Article	IF	CITATIONS
37	Solvothermal synthesis and good microwave absorbing properties for magnetic porous-Fe3O4/graphene nanocomposites. AIP Advances, 2017, 7, .	0.6	19
38	Controllable permittivity in 3D Fe ₃ O ₄ /CNTs network for remarkable microwave absorption performances. RSC Advances, 2017, 7, 26801-26808.	1.7	104
39	Hierarchical NiCo ₂ O ₄ /Co ₃ O ₄ /NiO porous composite: a lightweight electromagnetic wave absorber with tunable absorbing performance. Journal of Materials Chemistry C, 2017, 5, 3770-3778.	2.7	161
40	Surface-oxidized FeCo/carbon nanotubes nanorods for lightweight and efficient microwave absorbers. Materials and Design, 2017, 136, 13-22.	3.3	46
41	Magnetically Aligned Co–C/MWCNTs Composite Derived from MWCNT-Interconnected Zeolitic Imidazolate Frameworks for a Lightweight and Highly Efficient Electromagnetic Wave Absorber. ACS Applied Materials & Interfaces, 2017, 9, 30850-30861.	4.0	282
42	Porous CNTs/Co Composite Derived from Zeolitic Imidazolate Framework: A Lightweight, Ultrathin, and Highly Efficient Electromagnetic Wave Absorber. ACS Applied Materials & Interfaces, 2016, 8, 34686-34698.	4.0	427
43	Flaky FeSiAl alloy-carbon nanotube composite with tunable electromagnetic properties for microwave absorption. Scientific Reports, 2016, 6, 35377.	1.6	56
44	High-Frequency Absorption of the Hybrid Composites with Spindle-like Fe ₃ O ₄ Nanoparticles and Multiwalled Carbon Nanotubes. Nano, 2016, 11, 1650097.	0.5	8
45	Static and Dynamic Magnetization of Gradient FeNi Alloy Nanowire. Scientific Reports, 2016, 6, 20427.	1.6	28
46	Surfactant-free synthesis of octahedral ZnO/ZnFe2O4 heterostructure with ultrahigh and selective adsorption capacity of malachite green. Scientific Reports, 2016, 6, 25074.	1.6	44
47	Structure evolution of Prussian blue analogues to CoFe@C core–shell nanocomposites with good microwave absorbing performances. RSC Advances, 2016, 6, 105644-105652.	1.7	81
48	Clarifying the preferential occupation of Ga ³⁺ ions in YAG:Ce,Ga nanocrystals with various Ga ³⁺ -doping concentrations by nuclear magnetic resonance spectroscopy. Journal of Materials Chemistry C, 2016, 4, 10691-10700.	2.7	20
49	Effects of local structure of Ce3+ ions on luminescent properties of Y3Al5O12:Ce nanoparticles. Scientific Reports, 2016, 6, 22238.	1.6	109
50	Enhanced high-frequency absorption of anisotropic Fe3O4/graphene nanocomposites. Scientific Reports, 2016, 6, 25075.	1.6	69
51	Structural Formation and Improved Performances of Chemically Synthesized Composition-Controlled Micron-Sized Fe100â^'x Co x Particles. Journal of Superconductivity and Novel Magnetism, 2016, 29, 417-422.	0.8	5
52	Controlled Morphologies and Intrinsic Magnetic Properties of Chemically Synthesized Large-Grain FeCo Particles. Journal of Superconductivity and Novel Magnetism, 2015, 28, 1863-1869.	0.8	13
53	Flexible nanocomposites with enhanced microwave absorption properties based on Fe ₃ O ₄ /SiO ₂ nanorods and polyvinylidene fluoride. Journal of Materials Chemistry A, 2015, 3, 12197-12204.	5.2	165
54	Photocatalytic activity of Fe3O4/Bi2MoO6 composite in Rhodamine B decomposition. Journal of Applied Physics, 2015, 117, 17D709.	1.1	2

#	Article	IF	CITATIONS
55	High-frequency electromagnetic properties of the manganese ferrite nanoparticles. Journal of Applied Physics, 2015, 117, .	1.1	34
56	Size Influence to the High-Frequency Properties of Granular Magnetite Nanoparticles. IEEE Transactions on Magnetics, 2014, 50, 1-4.	1.2	4
57	Electromagnetic Properties of Co/Co ₃ O ₄ /Reduced Graphene Oxide Nanocomposite. IEEE Transactions on Magnetics, 2014, 50, 1-4.	1.2	2
58	Photocatalytic Activity of Magnetically Retrievable Bi ₂ WO ₆ /ZnFe ₂ O ₄ Adsorbent for Rhodamine B. IEEE Transactions on Magnetics, 2014, 50, 1-4.	1.2	1
59	Effect of Ti substitution on hydrogen storage properties of Zr1â´`xTixCo (x = 0, 0.1, 0.2, 0.3) alloys. Journal of Energy Chemistry, 2014, 23, 9-14.	7.1	68
60	Temperature-Driven Spin Reorientation Transition in CoPt/AlN Multilayer Films. Journal of Nanomaterials, 2012, 2012, 1-7.	1.5	0
61	Spin reorientation transition in (111) textured L10 CoPt layers. Applied Physics A: Materials Science and Processing, 2012, 109, 69-73.	1.1	4
62	Curie temperatures of CoPt ultrathin continuous films. Applied Physics A: Materials Science and Processing, 2012, 107, 519-523.	1.1	3
63	Roles of L1 ordering in controlling the magnetic anisotropy and coercivity of (111)-oriented CoPt ultrathin continuous layers in CoPt/AlN multilayer films. Journal of Applied Physics, 2011, 110, .	1.1	9
64	Magnetic and Microwave Absorption Properties of Core/Shell FeCo-Based Nanocomposites Synthesized by a Simple Wet Chemical Method. IEEE Transactions on Magnetics, 2011, 47, 3456-3459.	1.2	6
65	Synthesis and Physical Properties of Mn Doped ZnO Dilute Magnetic Semiconductor Nanostructures. Journal of Superconductivity and Novel Magnetism, 2011, 24, 699-704.	0.8	12
66	Effect of aspect ratio on microstructure and magnetic properties of spinel CoFe2O4 nanowire arrays. Applied Physics A: Materials Science and Processing, 2011, 105, 177-181.	1.1	7